Available online at www.sciencedirect.com
SCIENCE DIRECT®
Journal of Sound and Vibration 270 (2004) 813–832
JOURNAL OF SOUND AND VIBRATION
www.elsevier.com/locate/jsvi

Increased reliability of reference-based damage identification techniques by using output-only data

E. Parloo*, S. Vanlanduit, P. Guillaume, P. Verboven

Department of Mechanical Engineering, Vrije Universiteit Brussel, Pleinlaan 2, B-1050 Brussels, Belgium

Received 13 June 2002; accepted 24 January 2003

Abstract

During the past few years, a considerable number of damage identification techniques have been proposed and successfully tested on vibration data obtained from mechanical structures. Most vibration-based methods identify damage by interpreting measured changes in modal parameters. In practice, damage identification problems can occur due to minor changes in the boundary conditions of the test set-up especially if classic input–output vibration measurements are required for the diagnosis of a lightweight structure. In this contribution, a comparison is made between an input–output and output-only damage identification set-up for an aluminum beam structure suffering from fatigue-induced crack formation.

1. Introduction

During the past few years, a considerable number of damage identification techniques have been proposed and successfully tested on vibration data obtained from a wide range of mechanical structures [1]. Most techniques, for the identification of cracks, make use of an analytical model (e.g., finite element model) of the structure [2–11]. Other techniques aim for the same objective without making use of such models [12–15]. Until recently, some of these non-finite element model damage identification techniques were restricted to the domain of input–output data. For instance, the sensitivity-based technique, described in Ref. [15], and the changes in flexibility method [12] both require normalized mode shape estimates. Since the most straightforward normalization procedure of mode shapes involves the combined measurement of force and response at a driving point location [16], the application of such

*Corresponding author. Tel.: +32-2-629-2807; fax: +32-2-629-2865.
E-mail address: eli.parloo@vub.ac.be (E. Parloo).

0022-460X/03/$ - see front matter
doi:10.1016/S0022-460X(03)00494-2

techniques to output-only data was not evident. Recently, a new sensitivity-based normalization technique for output-only data was proposed and successfully tested [17,18]. The method allows the normalization of operational mode shape estimates, as obtained from output-only data, purely on a basis of output-only modal models. Combination of this method with the existing damage identification techniques, extends their applicability towards output-only data.

Most reference and vibration-based methods identify damage by interpreting measured changes in modal parameters (e.g., resonance frequencies, mode shape estimates, etc.). In practice, this assumption often makes the techniques vulnerable to the presence of errors in the identified modal parameters. A first example of such errors are stochastic uncertainties due to the presence of measurement noise on the data. In order to limit the possibility of obtaining false damage identification results due to this reason, accurate modal parameter estimates should be employed. Accurate estimates can, for instance, be obtained by means of a Maximum Likelihood estimator [19,20] that can take the noise information on the measurement data into account. Moreover, confidence intervals are generated with each estimation. This information can be used in order to objectively decide whether changes in modal parameters are statistically significant. Other sources of damage identification failure are caused by changes in modal parameters other than damage or stochastic uncertainty. For example, environmental changes (e.g., temperature changes, etc.) can also induce shifts in modal parameters of the same order of magnitude as structural defects [21,22]. For tests performed in laboratory conditions, small changes in the boundary conditions of a structure can cause similar changes in modal parameters. Small changes in the boundary conditions can, for instance, be caused by repeated assembling and disassembling of an experimental set-up built for off-line structural health monitoring measurements during a multi-step endurance testing. The chance of introducing such errors into the data sets are especially high if classical input–output vibration measurements are required for the diagnosis of relatively lightweight structures. For example, attaching a shaker or accelerometers to the device under test will not only induce a mass loading effect [23] but can also alter the boundary conditions of the set-up [24]. If these changes are wrongly interpreted as evidence of structural damage, false damage identification results (e.g., detection, localization, assessment) can be obtained or the effect of real defects can be masked by the changes in boundary conditions. The 'lighter' the structure, with respect to the excitation device, the more important such errors can become. Apart from a classic input–output set-up, another type of modal testing set-up is available for structural health monitoring purposes in laboratory conditions. Thanks to the output-only extension of the described damage identification techniques, use can be made of controlled laboratory free–free suspended experimental set-ups where the structure is excited acoustically and output-only response measurements are obtained by means of laser vibrometry. An important advantage to the use of such a set-up is that, apart from the suspension, all physical contact with the test structure is avoided and no additional changes in boundary conditions are induced due to the presence of excitation and/or acquisition devices. In this contribution, the benefits of using such an output-only experimental set-up over a classic input–output set-up involving lightweight structures will be investigated. For this purpose, the results of damage assessment experiments on a small aluminum beam structure, suffering from fatigue-induced crack formation, were compared. In order to increase the objectivity, multiple damage identification techniques (sensitivity-based, structural flexibility changes and strain energy method) were used.

2. Theoretical aspects

Some of the theoretical aspects used in this paper will be briefly discussed in the following sections.

2.1. Sensitivity of modal parameters

Some of the techniques used in this paper are based upon the calculation of sensitivities of modal parameters. As been shown in literature [25–29] many methods are available for the calculation of the sensitivity (derivatives) of eigenvalues and eigenvectors (such as modal parameters). In the case of a general viscous damped system, the sensitivity of modal parameters to local changes in mass, stiffness or damping, can be calculated by means of the estimated poles and normalized mode shapes without the use of a finite element model [16,30,31]. As an example, for a linear undamped system, the sensitivity of the natural frequency ω_i of mode i to a local change in mass in degree of freedom (d.o.f.) k is given by

$$\frac{\partial \omega_i}{\partial m_k} = -\omega_i \frac{\phi_{ki}^2}{2} \tag{1}$$

with ϕ_{ki} the d.o.f. k of the mass-normalized mode shape i, whereas the sensitivity of ω_i to a local change in stiffness between d.o.f.s p and q is given by

$$\frac{\partial \omega_i}{\partial k_{pq}} = \frac{(\phi_{pi} - \phi_{qi})^2}{2\omega_i}. \tag{2}$$

Similar expressions can be written for the sensitivity of mode shapes to local changes in mass or stiffness [16,30,31]. Moreover, damping can be taken into account by assuming a general viscous damped system. For real-life engineering structures with little damping present (normal mode shapes) and a predominant linear behavior, Eqs. (1) and (2) usually form a good approximation for the sensitivity of the estimated natural frequencies. In practice, errors will always be present on the identified modal parameters due to the presence of measurement noise (stochastic errors) on the data. For this reason, the uncertainty on the mass-sensitivities (calculated from Eq. (1)) will be lower than on the stiffness-sensitivities (calculated from Eq. (2)). In order to restrict the errors on the calculated sensitivities, the modal parameter estimates should be as accurate as possible. For this purpose, a Maximum Likelihood estimator [19,20] can for instance be used. This estimator is unbiased since it takes the noise information on the data into account [32]. The techniques employed in this paper exclusively make use of natural frequency sensitivity which can be computed without introducing 'truncation' errors. Calculating the sensitivity of a natural frequency only requires the natural frequency and mode shape of the considered mode. This can be considered as an advantage since the calculation of mode shape sensitivities involves the knowledge of all modes of the structure. In practice, only a limited number of modes can be experimentally determined. This fact introduces a 'truncation' error on the computed mode shape sensitivity.

Sensitivity analysis has proven to be extremely useful in several application domains [15,16,18,23,24,33]. The next section shortly introduces a sensitivity-based method for the normalization of mode shape estimates identified from output-only data.

2.2. Sensitivity-based normalization of output-only mode shape estimates

In Ref. [17], a sensitivity-based method was presented for the normalization of operational mode shape estimates obtained from output-only vibration data. Expressions (1) and (2) require the use of correctly normalized mode shape estimates. In the case of a classical forced-vibration test, where the input forces are measured, a full modal model of the structure can be determined. As long as a driving point measurement is performed, the obtained mode shape estimates can be scaled according to any normalization scheme desired [16]. During output-only vibration testing (e.g., in-operational modal analysis), only part of the modal model can be determined. Since the ambient forces that excite the structure are no longer being measured, the modal participation factors cannot be determined. As a result, the estimated mode shape vectors remain unscaled (i.e., dependant on the unknown level of ambient excitation) [34]. The relationship between the unscaled ($N_o \times 1$) mode shape vector $\{\psi\}_i$ (as obtained by output-only modal analysis) and the corresponding correctly normalized mode shape vector $\{\phi\}_i$ (as can be obtained from a classical forced-vibration test) of mode i can therefore be expressed by

$$\{\phi\}_i = \alpha_i \{\psi\}_i \tag{3}$$

with α_i an operational scaling factor for mode i dependant on the level of ambient excitation and N_o the number of outputs. The incompleteness of the modal model somewhat restricts its applicability to certain application domains [18,33]. The example of particular damage localization techniques (e.g., changes in structural flexibility method [1,12], sensitivity-based methods [15,33], etc.), which require the (mass-)normalized mode shapes of the monitored structure, show the need for a correct rescaling of the operational mode shapes. The basic idea behind the sensitivity-based normalization method is to use the sensitivity equations in order to assess the operational scaling factors α_i for each considered mode i. It is shown in Ref. [17], that operational mode shape estimates can be correctly rescaled on a basis of a controlled mass change experiment performed on the test structure. A first order approximation of the scaling factor α_i of a normal mode i can be found as

$$\alpha_i \simeq \sqrt{-\frac{2\Delta\omega_i}{\omega_i \sum_{k=1}^{N} (\psi_{ki})^2 \Delta m_k}} \tag{4}$$

with k the position of mass change Δm_k and N the number of mass changes used. The addition (or removal) of a small known mass Δm_k, in d.o.f. k of the test structure, will induce a change in natural frequencies between the original and the mass-loaded condition. The experimental determination of this change $\Delta\omega_i$, together with the in-operational modal model of the original structure, is sufficient to obtain an estimate of the operational scaling factor α_i. It should be noted that the change in natural frequency $\Delta\omega_i$ can be experimentally obtained from a single measurement in a well-chosen point of the structure. Some general guidelines concerning the use of suitable location(s) and mass(es) can be found in Refs. [17,33,35].

2.3. Damage identification techniques for use with output-only data

2.3.1. Detection of damage

Assume that a test structure remains stationary during a number of damage detection experiments and that changes in the condition of the structure are exclusively caused by the presence of structural defects. In that case, monitoring changes (shifts) in natural frequencies is an easy way to detect the presence of structural damage. Since the presence of stochastic uncertainty is inherent to performing measurements, statistical tools are required in order to objectively decide if shifts in natural frequencies are due to damage or measurement noise. For this purpose, 99.8% (3σ) confidence intervals can be calculated on the estimated natural frequencies. These stochastic uncertainty intervals can be directly obtained if a ML-estimator is used [19,20,36]. If the shifts between one (or more) natural frequencies of the reference and damage condition are statistically significant, a positive damage detection verdict is obtained.

In practice, environmental changes (e.g., temperature, etc.) can also induce shifts in natural frequencies (an other modal parameters) of the same order of magnitude as structural defects [21,22]. For tests performed in laboratory conditions, small changes in the boundary conditions of relatively lightweight structure, can cause similar changes in modal parameters. Small changes in the boundary conditions can, for instance, be caused by repeated assembling and disassembling of an experimental set-up built for off-line structural health monitoring measurements during a multi-step endurance testing. Since most vibration-based damage identification techniques rely upon the interpretation of changes in modal parameters, it is necessary to statistically discriminate shifts in modal parameters due to structural defects and shifts induced by changes other than damage (e.g, measurement noise, environmental and boundary conditions, etc.) [37].

2.3.2. Sensitivity-based damage identification for output-only data

Once the presence of structural damage is detected on a statistical basis, questions concerning the location and severity of the defects arise. The sensitivity-based damage assessment techniques, for use with output-only data, identify structural damage defined as local changes in mass or stiffness [33]. The sensitivity-based methods used in this contribution are based upon the interpretation of shifts in natural frequencies between a reference (undamaged) and a damaged condition. Both methods require the natural frequencies of the structure in its reference and damaged conditions as well as the normalized mode shape estimates from the structure in its reference condition. The first step for both methods will be the normalization of the output-only mode shape estimates of the test structure's reference condition. These normalized mode shape estimates are required for the calculation of the sensitivity of the natural frequencies from expressions (1) and (2) [33]. It should be noted that no finite element model of the test structure is required. Once this first task is performed, structural defects can be assessed by using the sensitivity of the natural frequencies to mass changes in structural d.o.f.s or stiffness changes between adjacent d.o.f.s. Although defects like formation of cracks are generally modelled as loss(es) in stiffness, this contribution will also consider the use of mass sensitivity for this purpose. One could argue that mass sensitivity could, to some approximated extent, also model stiffness changes due to the coupled nature of both types of structural modifications. As an example, a local change in stiffness could be introduced into a finite element model of a beam by lowering the cross-sectional area of one of the beam elements. Apart from the local change in stiffness,

a simultaneous local loss in mass would be obtained for that element. If the reference condition of a structure is altered by either a finite local change in mass or finite local change in stiffness, the following first order approximation can be written with respect to the chosen damage parameter P:

$$\{\mathbf{\Delta\omega}\} \simeq [\mathbf{S}] \cdot \{\mathbf{\Delta P}\} \tag{5}$$

with $\{\mathbf{\Delta\omega}\}$ the $(N_m \times 1)$ column vector with the shift in natural frequencies between the reference and damaged condition and $[\mathbf{S}]$ the $(N_m \times N_P)$ sensitivity matrix given by

$$[\mathbf{S}] = \begin{bmatrix} \frac{\partial\omega_1}{\partial P_1} & \frac{\partial\omega_1}{\partial P_2} & \cdots & \frac{\partial\omega_1}{\partial P_{N_P}} \\ \frac{\partial\omega_2}{\partial P_1} & \frac{\partial\omega_2}{\partial P_2} & \cdots & \frac{\partial\omega_2}{\partial P_{N_P}} \\ \vdots & \vdots & \ddots & \vdots \\ \frac{\partial\omega_{N_m}}{\partial P_1} & \frac{\partial\omega_{N_m}}{\partial P_2} & \cdots & \frac{\partial\omega_{N_m}}{\partial P_{N_P}} \end{bmatrix}. \tag{6}$$

The elements of the $(N_P \times 1)$ column vector $\{\mathbf{P}\}$ represents changes in mass at the corresponding N_p d.o.f.s or changes in stiffness between adjacent d.o.f.s. It should be noted that Eq. (5) is only valid if the finite changes can be considered small. Since we are interested in assessing structural damage as soon as possible, this poses no problem. By solving the inverse problem of Eq. (5) in a least-squares sense, damage information can be obtained from $\{\mathbf{\Delta P}\}$. The damage indices for this method are defined as the entries of $\{\mathbf{\Delta P}\}$. In practice, a pseudo-inverse can be used for solving this type of ill-conditioned system of equations [15]. This approach can result in damage indices that are distributed over the whole structure. A better localization of the defects can be obtained by using an iterative 'weighted' pseudo-inverse algorithm [38]

$$\{\mathbf{\Delta P(W)}\} = [\mathbf{W}]([\mathbf{S}][\mathbf{W}])^{+} \cdot \{\mathbf{\Delta\omega}\}, \tag{7}$$

where $[]^{+}$ denotes pseudo-inverse. The diagonal weighting matrix $[\mathbf{W}] = \mathrm{diag}(w_1, w_2, \ldots)$ is determined in such a way that the ℓ_p-norm of the damage indices is minimized:

$$K(\mathbf{W}) = \|\{\mathbf{\Delta P(W)}\}_i\|_p^p = \frac{1}{N_P} \sum_{i=1}^{N_P} |\Delta P_i|^p \tag{8}$$

with p a value close to zero (e.g., 0.01). Note that for $p \to 0$, the ℓ_p-norm $\|\{\mathbf{\Delta P(W)}\}\|_p^p$ converges to the number of entries in $\{\mathbf{\Delta P(W)}\}$ different from zero. Hence, minimizing Eq. (8) corresponds to making as many $\{\mathbf{\Delta P(W)}\}$ entries as possible equal to zero, i.e., find the solution requiring the lowest possible amount of locations. This corresponds to the idea that structural defects should be traced as early as possible while still small and present in limited number. Because the ℓ_p-norm is differentiable with respect to $[W]$, cost function (8) can be minimized by means of classical optimization algorithms [38].

Similar to the sensitivity-based techniques, the structural flexibility change method also requires mass-normalized mode shape estimates [12]. If confronted with output-only data, this method can also benefit from the sensitivity-based normalization procedure described above. By performing such a normalization for both the reference and damaged condition of the structure, the applicability of the modal flexibility change method can be extended to the domain of output-only

data. For this study, the differences in the diagonal values of the flexibility matrices before and after the damage are used as indicators of damage (damage indices) [39,40].

Other methods, such as the strain energy method [13,14], do not require normalized mode shape estimates because their damage indices are based on the calculation of a ratio. In this paper, the required curvature values were analytically calculated by making use of a cubic smoothing spline through the experimental mode shape estimates. It should be noted that a relatively high spatial resolution is required in order to obtain a reliable spline fit. The damage indices are defined in the same way as in Ref. [14].

3. Experimental set-up and results

In order to compare the suitability of the classic input–output and proposed output-only experimental set-up for damage identification purposes, both types of set-up were subjected to the following statistical reproducibility experiments before any damage was introduced into the beam. For the experiments, a $(480 \times 15 \times 2)$ mm aluminum beam was chosen with a total mass of 38×10^{-3} kg. During the statistical experiments, vibration responses of the beam were measured with a Polytec Scanning Laser Vibrometer in nine locations spread along the full length of the beam. In the output-only set-up, the beam was free–free suspended from a frame and acoustically excited at one end with a periodic chirp signal. This way, no contact was required with the beam for measurement or excitation purposes. A similar set-up was build for the input–output experiments, apart from the replacement of the acoustic excitation device by a shaker connected at the end of the beam. In this case, a clear connection between the artificial exciter and the test specimen is present allowing the possibility to introduce unwanted changes in boundary conditions of the structure. For the illustration (Fig. 1(b)), both experimental set-ups were assembled simultaneously with similar beams. In order to statistically investigate the effect of the experimental set-up on the natural frequencies of the beam, 10 data sets of measurements were

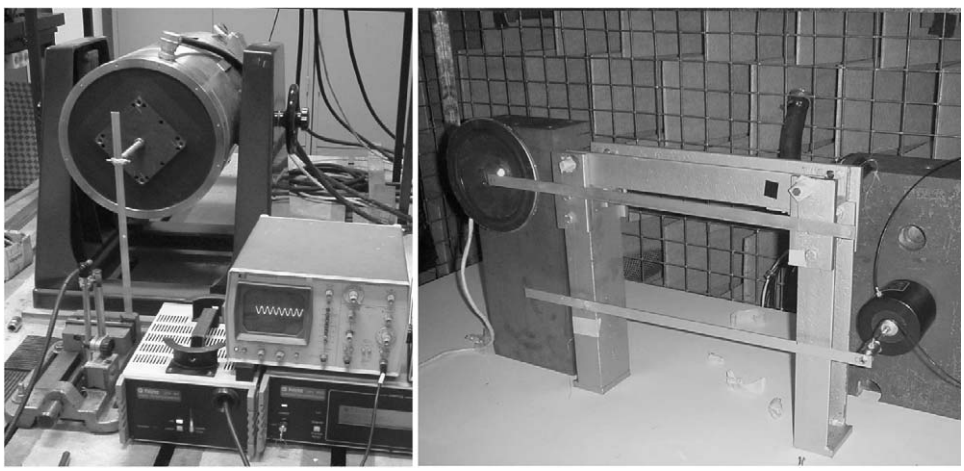

(a) (b)

Fig. 1. (a) Dynamic loading set-up. (b) Input–output and output-only experimental set-up.

performed. Each data set consists of nine subsequently performed measurements (1 for each grid point). In the case of the input–output set-up, the excitation force was measured as well. After obtaining every data set (nine measurements), the experimental set-up was broken down and reassembled for the next measurement (as would be the case during an off-line structural health monitoring experiment). Afterwards, the same statistical experiments were repeated (for both experimental set-ups) without disassembling/reassembling the set-up. For both experimental set-ups the natural frequencies and mode shape estimates of the first six modes of the beam were identified with a Maximum Likelihood (ML) estimator [19,20] for every obtained data set. This model based system identification technique is able to take noise information on the data into account. Moreover, confidence intervals (with respect to the stochastic measurement uncertainty) on the identified modal parameters are generated with each estimation procedure. This way, shifts in natural frequency can be statistically classified as either caused by a true change in condition (e.g., boundary condition change, presence of defect(s), etc.) of the structure or simply due to the presence of noise on the measurements.

Tables 1 and 2 give an overview of the obtained results for both types of experimental set-up. Apart from the first six natural frequencies, the tables also include the 99.8% confidence intervals in case of an untouched experimental set-up ($3\sigma_1$) and repeated reassembling of the set-up ($3\sigma_{exp}$). By comparing the results from Tables 1 and 2, a few important conclusions can be drawn. In general, a much larger test-to-test variability is obtained, for both input–output and output-only set-ups, if the set-up is dissassembled/reassembled between measuring data sets instead of being left untouched. However, comparing the $3\sigma_{exp}$ results for both tables clearly shows that

Table 1
Results from statistic analysis for output-only experimental set-up

Mode	ω (rad/s)	$3\sigma_1$ (rad/s)	$3\sigma_1$ (%)	$3\sigma_{exp}$ (rad/s)	$3\sigma_{exp}$ (%)
1	273.78	0.27	0.099	1.65	0.604
2	762.08	0.10	0.013	0.68	0.089
3	1493.76	0.15	0.010	1.20	0.080
4	2466.15	0.22	0.009	0.70	0.028
5	3681.64	0.34	0.009	1.23	0.033
6	5140.75	0.46	0.009	1.75	0.034

Table 2
Results from statistic analysis for input–output experimental set-up

Mode	ω (rad/s)	$3\sigma_1$ (rad/s)	$3\sigma_1$ (%)	$3\sigma_{exp}$ (rad/s)	$3\sigma_{exp}$ (%)
1	143.38	0.38	0.260	3.15	2.194
2	381.89	0.06	0.015	12.86	3.367
3	782.57	0.49	0.063	5.48	0.700
4	881.17	2.99	0.341	7.90	0.896
5	1326.96	1.68	0.127	3.49	0.263
6	1856.04	2.11	0.114	5.23	0.282

reassembling the output-only set-up has much less influence on the identified natural frequencies than reassembling the input–output set-up. The input–output set-up therefore has a larger probability of masking small changes in natural frequency due to actual defects. This outcome could be expected since, apart from the suspension, the input–output set-up still has an additional boundary condition with the artificial excitation device. This makes the input–output set-up more valuable to small changes in boundary conditions during a repeated disassembly/reassembly of the measurement set-up. The same conclusion can be drawn from Figs. 2 and 3 representing the results from all the data set obtained with reassembly ('△') plotted against the one without reassembly ('o') for modes 2–3. For each result the 99.8% confidence interval, generated by the ML estimator, is indicated by an error bar. The slightly increasing trend visible for the 'untouched' experiments of the output-only set-up can be due to a slight temperature instability (about 1°C variation) of the measurement room.

After the statistical analysis, experiments were performed for the identification of cracks induced by fatigue in the aluminum beam. The formation and growth of localized cracks was accomplished by clamping the beam on one end and exciting it by means of a large shaker. As an excitation signal, a sine wave was used with a frequency near the first resonance of the structure in these conditions (Fig. 1(a)). This way, after 30 min of dynamic loading, localized fatigue-induced

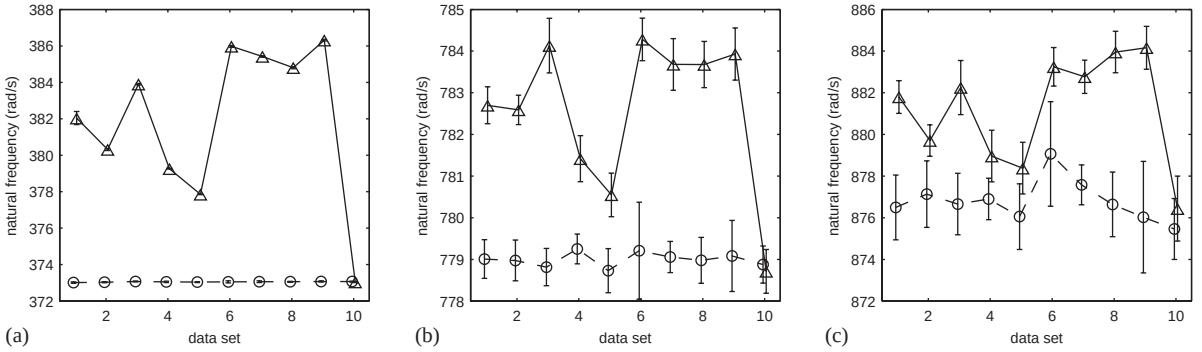

Fig. 2. Shifts in resonance frequencies for statistical tests—input–output set-up: repeated reassembly '△', untouched 'o'.

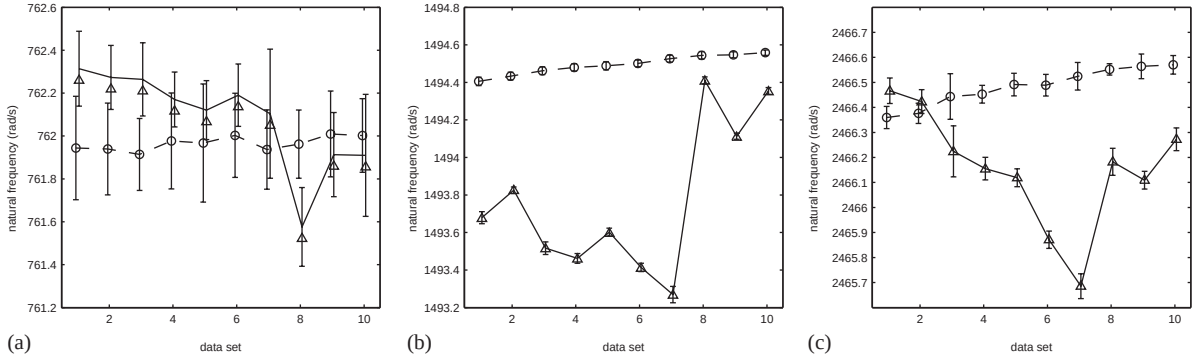

Fig. 3. Shifts in resonance frequencies for statistical tests—output-only set-up: repeated reassembly '△', untouched 'o'.

cracks appeared in the beam exclusively near the connection with the shaker. A reference (undamaged) and four damage cases with increasing severity were considered. Each damage case was obtained by further dynamic loading (by sine excitation) of the beam in its previous condition. By normal visual inspection, it was only possible to detect the cracks in the last two (and most severe) levels of damage (even if the location of the damage was known beforehand). By making use of the liquid penetration technique [41] (with a Magnaflux ZL37 sensitivity class 4 penetrant) the cracks could be visualized for all four levels of damage (Fig. 4). No cracks were found in the reference condition of the beam. During each stage (including the reference condition), the beam was measured in both the input–output and output-only measurement set-up. Response measurements were made with the Scanning Laser Vibrometer in 31 equidistant points (d.o.f.s) along the full length of the beam. The cracks were located near d.o.f. 6. For the input–output experimental set-up, a driving point measurement was used for the mass-normalization of the mode shape estimates of the specimen in all of its damage conditions. For the output-only case, the sensitivity-based normalization procedure was used with a 6×10^{-4} kg mass change (ca. 1.5% of the total weight of the beam) in d.o.f. 1 for all damage levels.

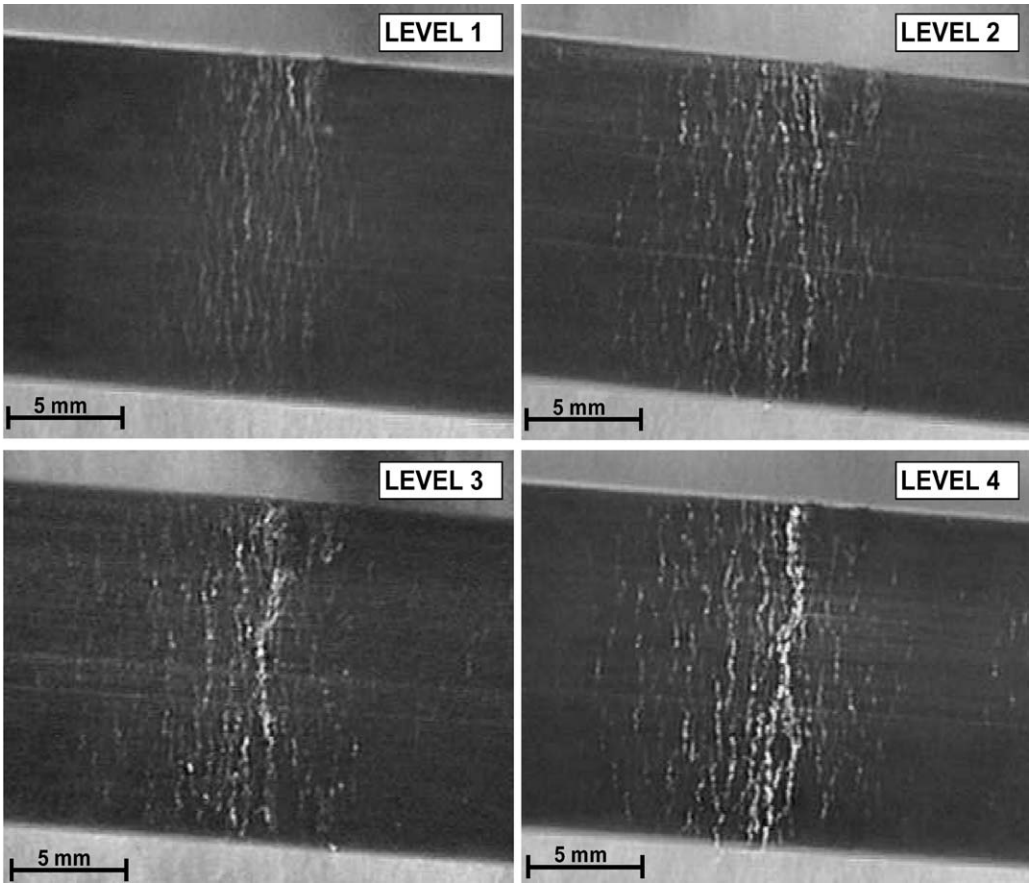

Fig. 4. Pictures of the different stages of crack damage: levels 1–4.

The relative shifts in natural frequency for the four damage cases, for the output-only set-up, are depicted in Fig. 5 for modes 2–4. For each presented damage level, the figures include the 99.8% confidence intervals (under the form of very small error bars) reflecting the stochastic uncertainty of the measurement. Each figure also indicates the confidence interval (dashed lines) reflecting the repeated reassembling of the experimental test set-up (summed up by the stochastic confidence interval of the reference measurement—small enough to be discarded in this case) denoted by $+3\sigma$ and -3σ. All values that fall out of this reference confidence interval will be considered as statistical significant shifts due to the presence of structural defects. The relative shifts of modes 3 and 4 can be considered as statistically significant for all damage cases. This means that, in case the output-only set-up is used, all damage cases can be detected on a statistical base. The latter is no longer true for the input–output set-up. In this case, only levels 3 and 4 can be considered as statistically significant (Fig. 6) due to the fact that changes in boundary conditions are masking the effect of the actual structural defect. Taking higher frequency modes into account did not improve the detection resolution for this case.

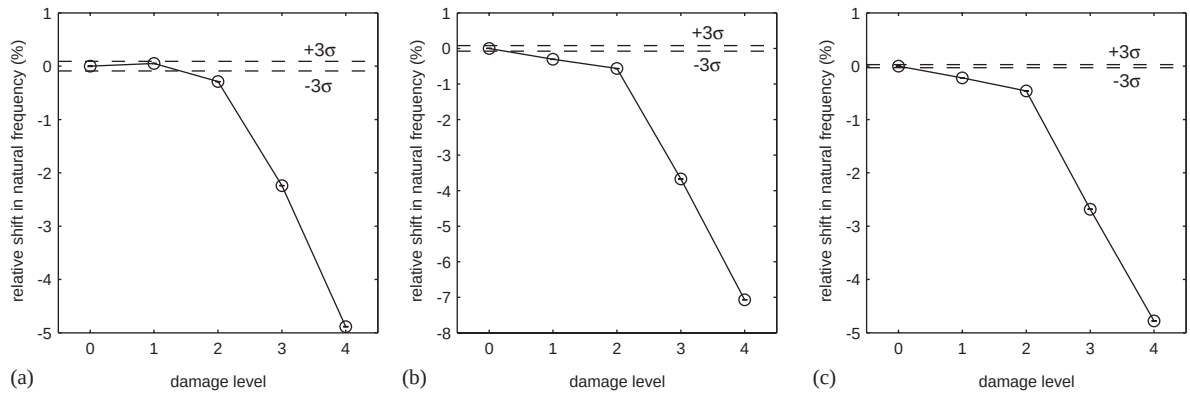

Fig. 5. Relative shifts in natural frequency versus damage level—output-only experimental set-up: modes 2(a), 3(b) and 4(c).

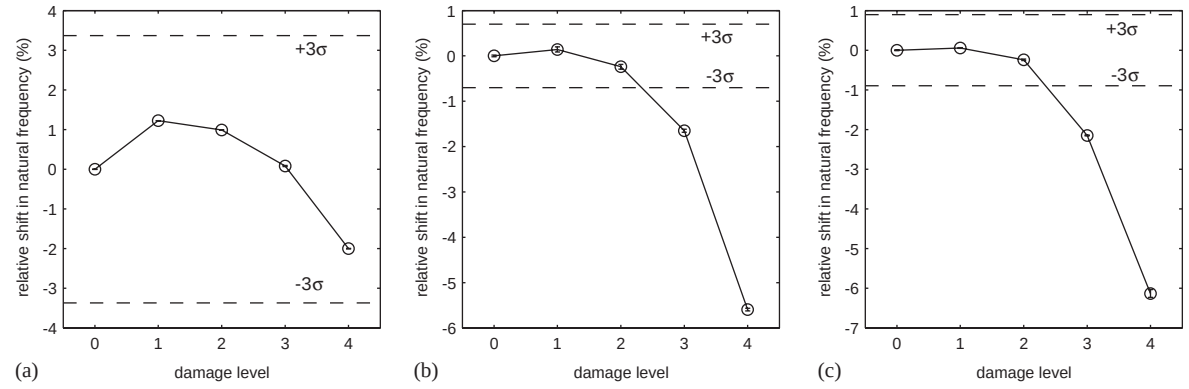

Fig. 6. Relative shifts in natural frequency versus damage level—input–output experimental set-up: modes 2(a), 3(b) and 4(c).

Next, attention was focused on the localization of the cracks introduced into the test specimen. The described damage localization techniques (see Section 2.3) were used in combination with both the input–output and output-only experimental set-up for the identification of the different levels of damage. Figs. 7 and 8 show the results of the stiffness sensitivity-based method for the output-only experimental set-up. All sensitivity-based damage localization results in this paper are based on the use of the first six modes. Taking more modes into consideration did not improve the results. The results in Fig. 7 were obtained by using a classic pseudo-inverse approach for solving Eqs. (5). The high-magnitude of the damage indices found for element 5, indicating a change in stiffness between d.o.f.s 5 and 6, correctly localizes the presence of the defects for all four levels of damage. Element 26 (between d.o.f.s 26 and 27), situated on the symmetric position of the actual damage location, is also identified as a damage location. This can be explained by the highly symmetric form of the test specimen and the fact that shifts in natural frequencies were used.

A drawback of using a classic pseudo-inverse is the fact that the identified solutions are 'smeared' out over all damage indices of the test structure. In order to avoid this, an iteratively weighted pseudo-inverse approach can be used for solving Eq. (5). The results found with the latter approach are presented in Fig. 8. For damage level 1, the structural defect can be correctly localized. Moreover, the false symmetric damage location (at element 26) is no longer indicated. For damage levels 2–4, the method decides on the symmetric location rather than on the true

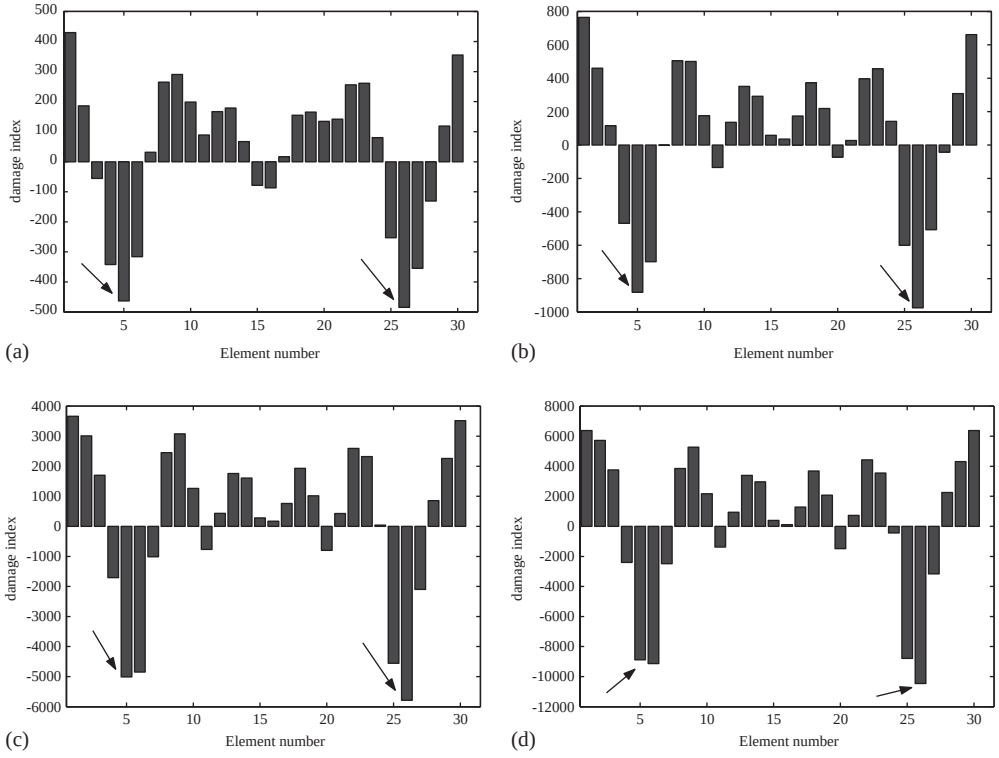

Fig. 7. Pseudo-inverse results from the stiffness sensitivity-based methods—output-only experimental set-up: damage levels 1(a), 2(b), 3(c) and 4(d).

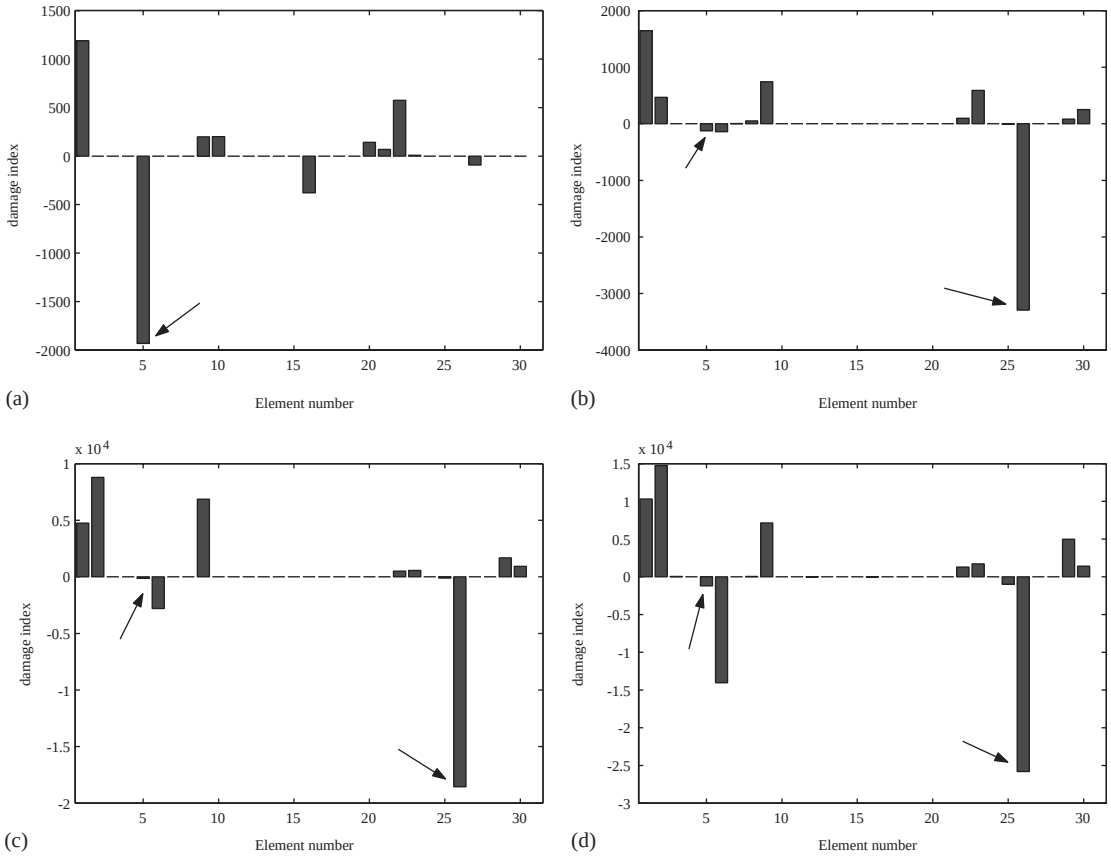

Fig. 8. Weighted pseudo-inverse results from the stiffness sensitivity-based methods—output-only experimental set-up: damage levels 1(a), 2(b), 3(c) and 4(d).

damage location. As explained in Section 2.3.2, the weighted pseudo-inverse approach minimizes cost function (8). This approach corresponds to making as many damage indices as possible equal to zero, i.e., find the solution that requires the lowest possible amount of damage locations. If the beam structure had been perfectly symmetric and no (stochastic and systematic) errors present in the natural frequency and mode shape estimates, the weighted pseudo-inverse approach would yield a symmetric damage index diagram. In that case, the true damage location cannot be discriminated from the position located symmetric to the damage on a basis of shifts in natural frequencies. In the real case, both the mode shape and natural frequency estimates are contaminated with stochastic errors (due to measurement noise) and systematic errors (e.g., due to small changes in boundary conditions between the different measurements). Since the mode shapes are highly symmetric (see Fig. 9), these small errors in natural frequency shifts can easily allow a better minimization of the cost function for the true or the false symmetric damage location than the solution where the damage is divided equally between the true and symmetric damage location. Although the beam is symmetric, the presence of the uncertainties will create a false asymmetry of the damage identification problem and allow the algorithm to prefer either the

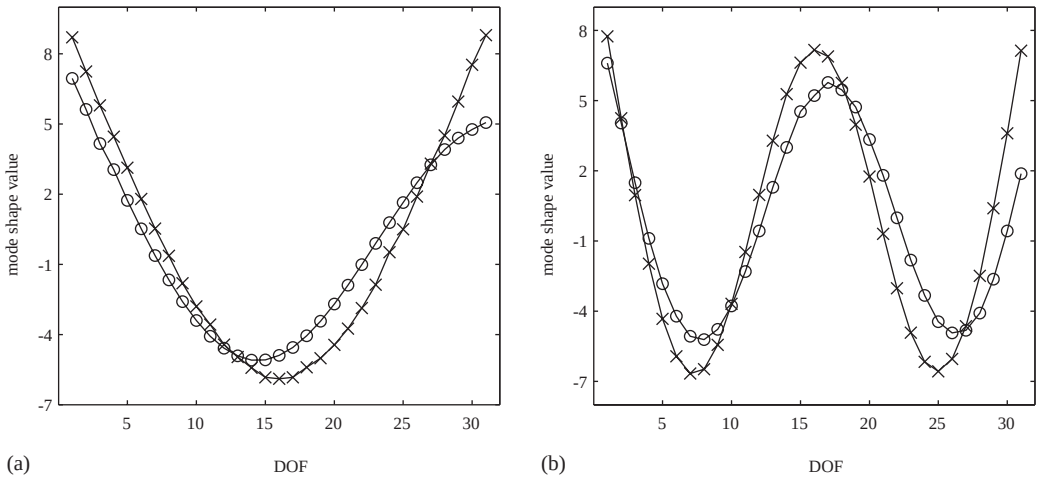

Fig. 9. Mode shape estimates of the reference condition for modes 1(a) and 3(b): obtained with output-only set-up '×' and input–output set-up '○'.

true or false symmetric damage location. A solution to this apparent erroneous damage localization can consist in making an a priori hypothesis on the location of the defect. In this case, it is sufficient to assume that the structural defect is located in the first half of the beam. The results can then be transformed by adding each of the damage indices in the first half of the beam to their corresponding symmetric damage index on the other half. The use of such an operation and a priori hypothesis allows a correct localization of the crack for all damage cases. It should be noted that, for more asymmetrical test structures these symmetry problems are usually avoided [17].

Since the effects of mass and stiffness modifications to a structure are coupled, the mass sensitivity-based approach was tried out as well. For this simple case, the modelling of a loss in stiffness by means of 'apparent' mass changes was successful. The results for the output-only set-up are shown in Fig. 10. For the first damage level, the sensitivity-based method correctly indicates the position of the cracks (near d.o.f. 6). For damage levels 2–4, the method indicates d.o.f. 7, being the position adjacent to the crack location. It should be noted that, as far as we know, the formation of the cracks did not induce a genuine loss of mass (material) from the beam (as would be the case for a saw cut). The damage locations found with the mass sensitivity-based method are in good agreement with those found with the strain energy method. Results show that, for the output-only set-up, the strain energy method correctly indicates d.o.f.s 6 and 7 as damage locations for levels 2–4 (Fig. 11(b)–(d)). However, for the first damage level, the correct location of the cracks can no longer be objectively identified (Fig. 11(a)). The change in flexibility method was only able to correctly localize the cracks for damage levels 3 and 4 if the high damage indices at the edges of the beam are discarded (Fig. 12). Seven modes were taken into account for both the strain energy and changes in structural flexibility method. Increasing the number of modes did not improve the damage identification results in any of the cases.

In the case of the input–output experimental set-up, the sensitivity-based methods (both stiffness and mass sensitivity) are only able to localize the damage in the last two cases (Figs. 13 and 14). It should be noted that this observation is in agreement with the damage

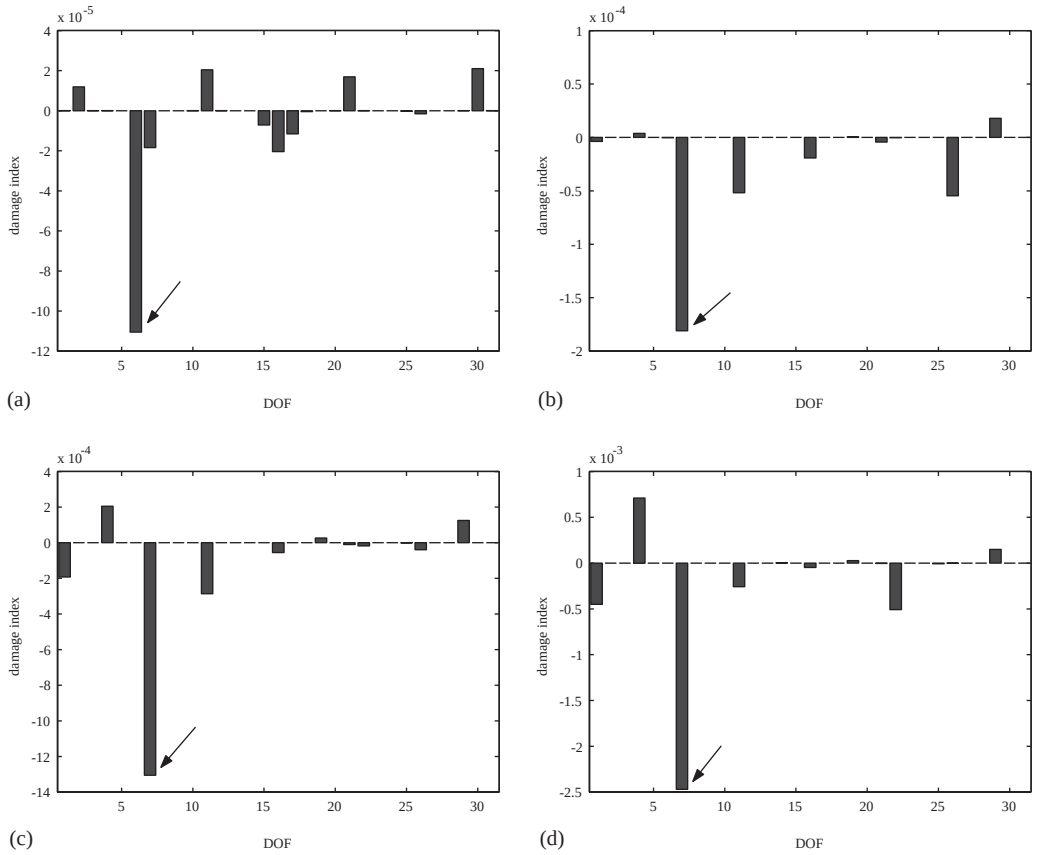

Fig. 10. Weighted pseudo-inverse results from the mass sensitivity-based method—output-only experimental set-up: damage levels 1(a), 2(b), 3(c) and 4(d).

detection results shown in Fig. 6. These results show that for damage levels 1 and 2, the shift in natural frequencies due to structural defects can no longer be discriminated, on a statistical basis, from the shifts due to small changes in boundary conditions. As mentioned before, these small boundary condition changes are induced by the repeated assembly/disassembly of the input–output measurement set-up in between the dynamic loading stages (fatigue experiment) of the test specimen. This time, the results of the stiffness sensitivity-based method Fig. 13 has less trouble with false damage indications at the position symmetric to the actual damage site than the results for the mass sensitivity-based method. Compared to the results obtained with the output-only set-up, the sensitivity-based input–output damage identification results seem superior for the more severe damage cases 3 and 4. For both cases, the true damage location is indicated instead of the symmetric position on the beam. Although the beam on itself is symmetric, the system under test, which is the beam influenced by the exciter connection, is no longer symmetric. Contrary to the output-only set-up, this asymmetry is not caused by the presence of small stochastic or systematic errors but rather by a strong structural modification due to the presence of the exciter connection (mass loading effect of the measurement transducer). This last fact is confirmed by the clear asymmetry of the identified mode shapes (Fig. 10). This latter asymmetry, turns the damage

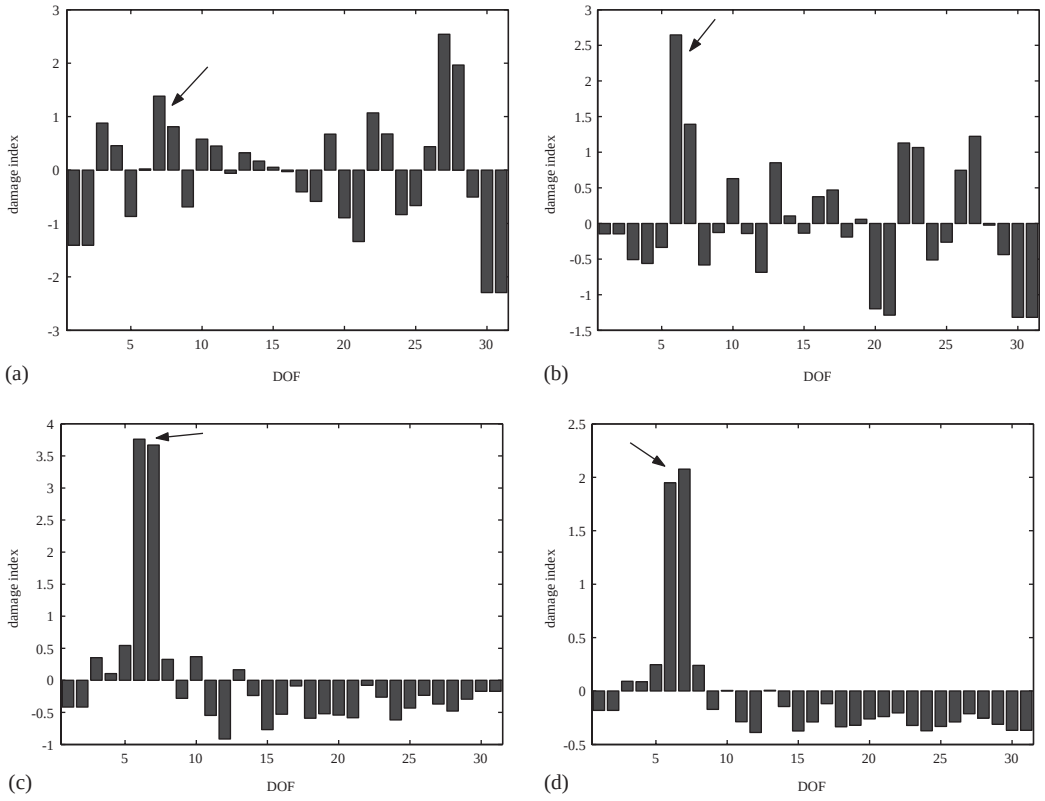

Fig. 11. Results from the strain energy method—output-only experimental set-up: damage levels 1(a), 2(b), 3(c) and 4(d).

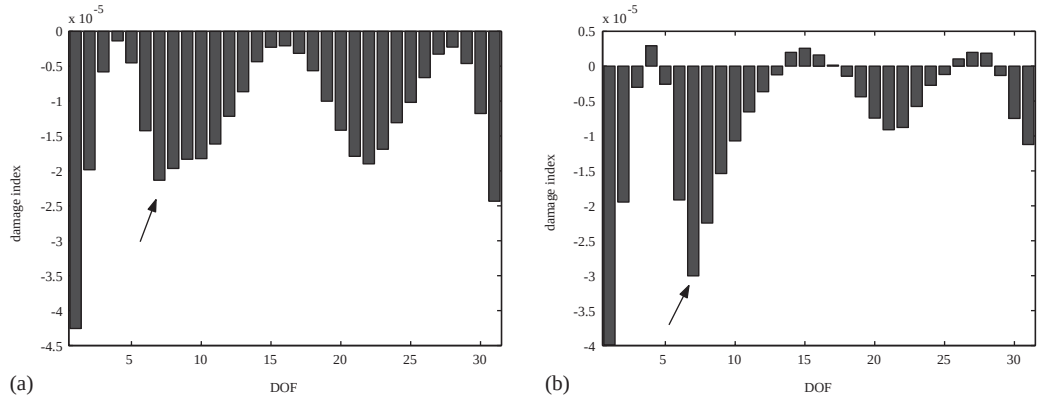

Fig. 12. Results from the changes in modal flexibility method—output-only experimental set-up: damage levels 3(a) and 4(b).

identification into an true asymmetric problem that no longer suffers from symmetry induced trouble as was encountered in the symmetric output-only case. The unfavorable influence of using the input–output set-up for the early detection and identification of cracks is confirmed by the

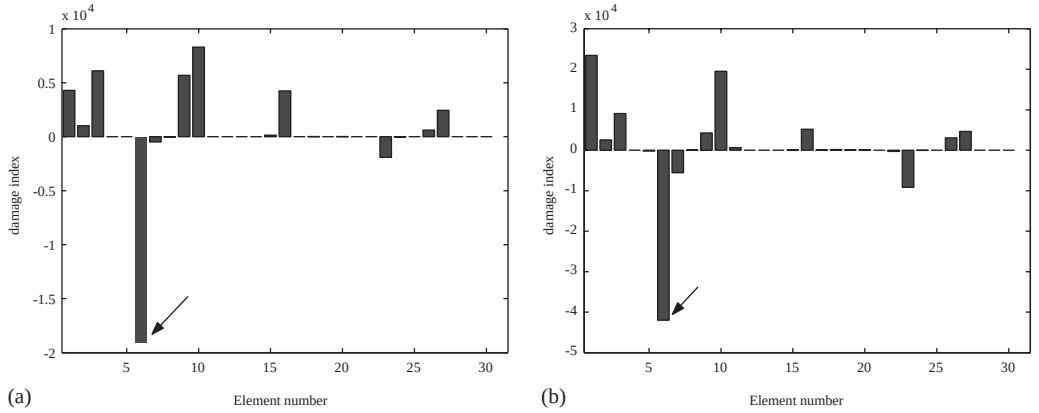

Fig. 13. Weighted pseudo-inverse results from the stiffness sensitivity-based method—input–output experimental set-up: damage levels 3(a) and 4(b).

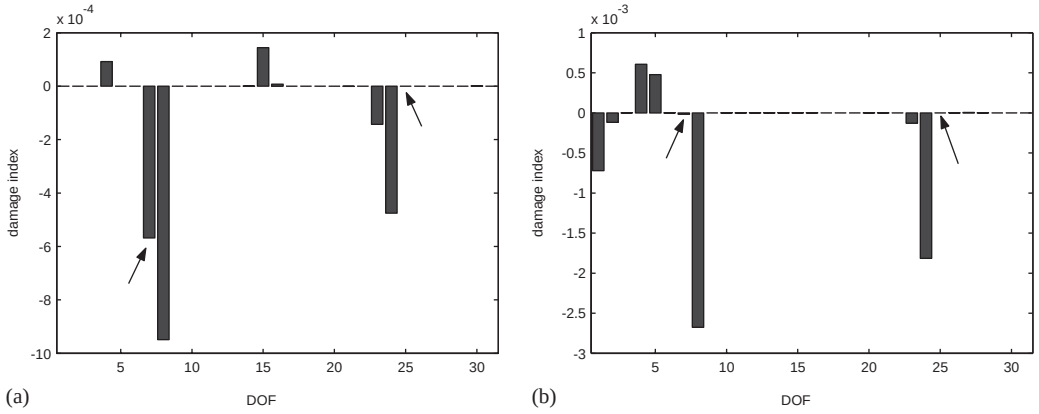

Fig. 14. Weighted pseudo-inverse results from the mass sensitivity-based method—input–output experimental set-up: damage levels 3(a) and 4(b).

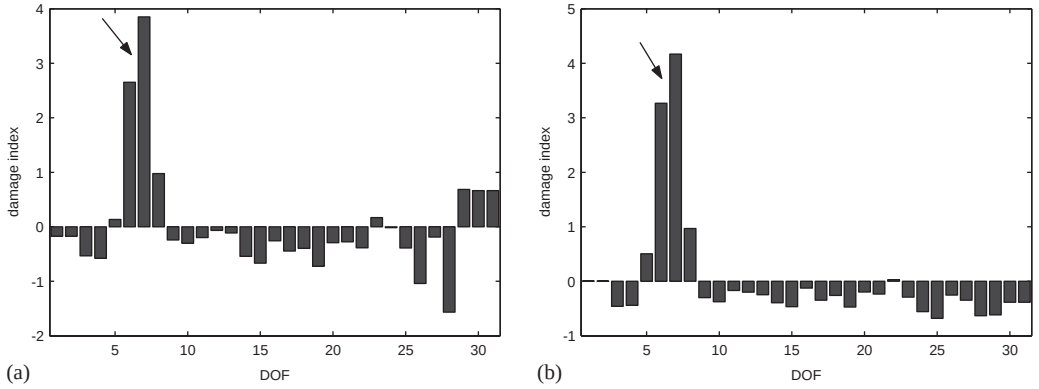

Fig. 15. Results from the strain energy method—input–output experimental set-up: damage levels 3(a) and 4(b).

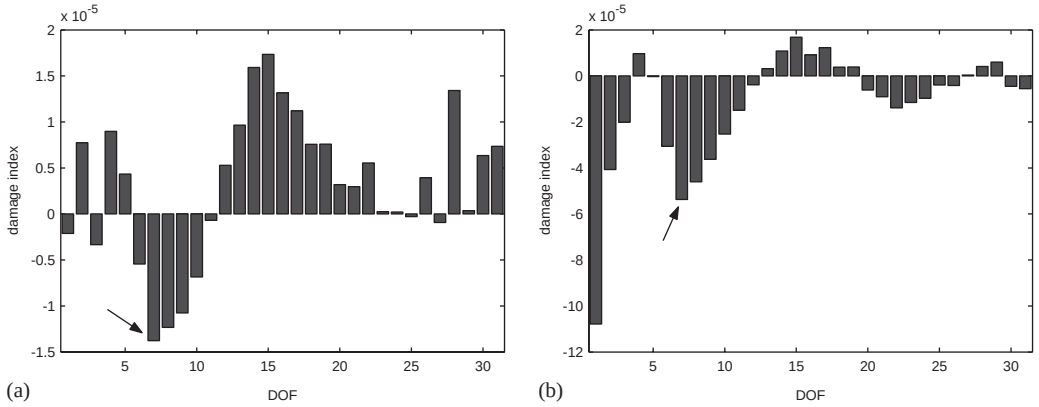

Fig. 16. Results from the changes in modal flexibility method—input–output experimental set-up: damage levels 3(a) and 4(b).

results of both strain energy and changes in structural flexibility method. The strain energy method is only able to correctly identify the last two levels of damage (Fig. 15). The changes in structural flexibility method only succeeds in correctly identifying the last and most severe level of damage (Fig. 16).

4. Conclusions

In this contribution, a comparison was made between a classic input–output experimental set-up and an output-only one for laboratory-condition damage identification. A statistical analysis shows that disassembling/reassembling the output-only set-up has much less influence on the identified natural frequencies of the structure under test than on the classic input–output set-up. The latter therefore has a larger probability of masking small changes in natural frequency due to actual defects. The results from the statistical analysis are supported by the damage localization results of three independent damage identification techniques. In this study, the sensitivity-based methods were found to be the most sensitive techniques for the identification of fatigue-induced crack growth in the used aluminum beam.

Acknowledgements

This research has been supported by the Fund for Scientific Research—Flanders (Belgium) (FWO), the Institute for the Promotion of Innovation by Science and Technology in Flanders (IWT) and by the Research Council (OZR) of the Vrije Universiteit Brussel (VUB).

References

[1] S. Doebling, C. Farrar, Computation of structural flexibility for bridge health monitoring using ambient modal data, *Proceedings of the 11th ASCE Engineering Mechanics Conference*, Ft. Lauderdale, FL, 1996, pp. 1114–1117.

[2] R. Adams, P. Cawley, C. Pye, B. Stone, A vibration technique for non-destructively assessing the integrity of structures, *Journal of Mechanical Engineering Science* 20 (2) (1978) 93–100.
[3] P. Gudmundson, The dynamic behaviour of slender structures, *Journal of Mechanics and Physics of Solids* 31 (4) (1983) 329–345.
[4] G. Hearn, R. Testa, Modal analysis for damage detection in structures, *Journal of Structural Engineering* 117 (10) (1991) 3042–3063.
[5] R. Liang, J. Hu, F. Choy, Theoretical study of crack-induced eigenfrequency changes on beam structures, *Journal of Engineering Mechanics, American Society of Civil Engineers* 118 (2) (1992) 384–396.
[6] D. Zimmerman, M. Kaouk, Structural damage detection using a minimum rank update theory, *Journal of Vibration and Acoustics* 116 (2) (1994) 222–230.
[7] Y. Narkis, Identification of crack location in vibrating simply supported beams, *Journal of Sound and Vibration* 172 (4) (1994) 549–558.
[8] F. Vestroni, D. Capecchi, Damage evaluation in cracked vibrating beams using experimental frequencies and finite element models, *Journal of Vibration and Control* 2 (1996) 69–86.
[9] R. Ruotolo, C. Surace, Damage assessment of multiple cracked beams: numerical results and experimental validation, *Journal of Sound and Vibration* 206 (4) (1997) 567–588.
[10] A. Morassi, Identification of a crack in a rod based on changes in pairs of natural frequencies, *Journal of Sound and Vibration* 242 (4) (2001) 577–596.
[11] J. Sinha, M. Friswell, S. Edwards, Simplified models for the location of cracks in beam structures using measured vibration data, *Journal of Sound and Vibration* 251 (1) (2002) 13–38.
[12] A. Pandey, M. Biswas, Damage detection in structures using changes in flexibility, *Journal of Sound and Vibration* 169 (1) (1994) 3–17.
[13] N. Stubbs, J. Kim, K. Topole, An efficient and robust algorithm for damage localization in offshore platforms, *Proceedings of the ASME 10th Structures Congress*, 1992, pp. 543–546.
[14] P. Cornwell, S. Doebling, C. Farrar, Application of the strain energy damage detection method to plate-like structures, *Journal of Sound and Vibration* 224 (2) (1999) 359–374.
[15] E. Parloo, P. Guillaume, M. Van Overmeire, Damage assessment using mode shape sensitivities, *Mechanical Systems and Signal Processing* 17 (3) (2003) 499–518.
[16] W. Heylen, S. Lammens, P. Sas, *Modal Analysis Theory and Testing*, Department of Mechanical Engineering, Katholieke Universiteit Leuven, Leuven, Belgium, 1995.
[17] E. Parloo, P. Verboven, P. Guillaume, M. Van Overmeire, Sensitivity-based operational mode shape normalization, *Mechanical Systems and Signal Processing* 16 (5) (2002) 757–767.
[18] E. Parloo, P. Verboven, P. Guillaume, M. Van Overmeire, Force identification by means of in-operation modal models, *Journal of Sound and Vibration* 262 (1) (2003) 161–173.
[19] P. Guillaume, P. Verboven, S. Vanlanduit, Frequency-domain maximum likelihood estimation of modal parameters with confidence intervals, *Proceedings of the 23rd International Seminar on Modal Analysis (ISMA23)*, Leuven, Belgium, September 1998, pp. 359–366.
[20] P. Guillaume, L. Hermans, H. Van der Auweraer, Maximum likelihood identification of modal parameters from operational data, *Proceedings of the 17th International Modal Analysis Conference (IMAC17)*, Orlando, FL, February 1999, pp. 1887–1893.
[21] B. Peeters, G. De Roeck, One-year monitoring of the z24-bridge: environmental effects versus damage events, *Earthquake Engineering and Structural Dynamics* 30 (2) (2001) 149–171.
[22] B. Peeters, J. Maeck, G. De Roeck, Vibration-based damage detection in civil engineering: excitation sources and temperature effects, *Smart Materials and Structures* 10 (3) (2001) 518–527.
[23] H. Van der Auweraer, W. Leurs, P. Mas, L. Hermans, Modal parameter estimation from inconsistent data sets, *Proceedings of the 18th International Modal Analysis Conference (IMAC18)*, San Antonio, TX, 2000, pp. 763–771.
[24] B. Cauberghe, P. Guillaume, B. Dierckx, Identification of modal parameters from inconsistent data, *Proceedings of the 20th International Modal Analysis Conference (IMAC20)*, Los Angeles, CA, 2002.
[25] R. Fox, M. Kapoor, Rates of change of eigenvalues and eigenvectors, *American Institute of Aeronautics and Astronautics Journal* 6 (12) (1968) 2426–2429.

[26] L. Rogers, Derivatives of eigenvalues and eigenvectors, *American Institute of Aeronautics and Astronautics Journal* 8 (1970) 943–944.
[27] R. Plaut, K. Huseyin, Derivatives of eigenvalues and eigenvectors in non-self-adjoint systems, *American Institute of Aeronautics and Astronautics Journal* 11 (2) (1973) 250–251.
[28] C. Rudisill, Derivatives of eigenvalues and eigenvectors for a general matrix, *American Institute of Aeronautics and Astronautics Journal* 12 (5) (1974) 721–722.
[29] R. Nelson, Simplified calculation of eigenvector derivatives, *American Institute of Aeronautics and Astronautics Journal* 14 (9) (1976) 1201–1205.
[30] P. Vanhonacker, Differential and difference sensitivities of natural frequencies and mode shapes of mechanical structures, *American Institute of Aeronautics and Astronautics Journal* 18 (12) (1980) 1511–1514.
[31] P. Vanhonacker, The Use of Modal Parameters of Mechanical Structures in Sensitivity Analysis-, System Synthesis- and System Identification Methods. Ph.D. Thesis, Department of Mechanical Engineering, Katholieke Universiteit Leuven, 1988.
[32] R. Pintelon, J. Schoukens, *System Identification: a Frequency-domain Approach*, IEEE Press, New York, 2001.
[33] E. Parloo, P. Verboven, P. Guillaume, M. Van Overmeire, Autonomous structural health monitoring—part II: vibration-based in-operation damage assessment, *Mechanical Systems and Signal Processing* 16 (4) (2002) 659–675.
[34] E. Parloo, P. Verboven, P. Guillaume, M. Van Overmeire, Maximum likelihood identification of modal parameters from non-stationary operational data, *Proceedings of the 19th International Modal Analysis Conference (IMCAC19)*, Orlando, FL, 2001, pp. 425–431.
[35] E. Parloo, P. Verboven, P. Guillaume, M. Van Overmeire, Iterative calculation of non-linear changes by first order approximations, *Proceedings of the 20th International Modal Analysis Conference (IMAC20)*, Los Angeles, CA, 2002, pp. 1084–1090.
[36] R. Pintelon, P. Guillaume, Y. Rolain, J. Schoukens, H. Van Hamme, Parametric identification of transfer function in the frequency domain—a survey, *IEEE Transactions on Automatic Control* 39 (11) (1994) 2245–2260.
[37] B. Peeters, G. de Roeck, One year monitoring of the z24-bridge: Environmental effects versus damage events, *Proceedings of the 18th International Modal Analysis Conference (IMAC18)*, San Antonio, TX, 2000, pp. 1570–1576.
[38] P. Guillaume, E. Parloo, P. Verboven, G. De Sitter, An inverse method for the identification of localized excitation sources, *Proceedings of the 20th International Modal Analysis Conference (IMAC20)*, Los Angeles, CA, 2002.
[39] S. Doebling, C. Farrar, Statistical damage identification techniques applied to the i-40 bridge over the rio grande river, *Proceedings of the 16th International Modal Analysis Conference (IMAC16)*, Santa Barbara, CA, 1998, pp. 1717–1724.
[40] N. Robinson, L. Peterson, G. James, S. Doebling, Damage detection in aircraft structures using dynamically measured static flexibility matrices, *Proceedings of the 14th International Modal Analysis Conference (IMAC14)*, Dearborn, MI, 1996, pp. 857–865.
[41] W. McGonnagle, *Nondestructive Testing*, 2nd Edition, Gordon and Breach, London, 1961.